Spectrochimica Acta Part B 124 (2016) 109–115

Contents lists available at ScienceDirect

Spectrochimica Acta Part B

journal homepage: www.elsevier.com/locate/sab

Technical note

Practical guidelines for best practice on Total Reflection X-ray Fluorescence spectroscopy: Analysis of aqueous solutions

Sofía Riaño, Mercedes Regadío, Koen Binnemans, Tom Vander Hoogerstraete *

KU Leuven, Department of Chemistry, Celestijnenlaan 200F, 3001 Heverlee, Belgium

ARTICLE INFO

Article history:
Received 26 May 2016
Received in revised form 5 September 2016
Accepted 5 September 2016
Available online 06 September 2016

Keywords:
TXRF
Sample preparation
Aqueous samples
TXRF calibration

ABSTRACT

Despite the fact that Total Reflection X-ray Fluorescence (TXRF) is becoming more and more popular as a quantification technique in analytical chemistry due to its simplicity and robustness, there are still some key aspects related to the sample preparation that need to be improved. In this work, the effect of different parameters is investigated: measurement time, carrier position, sample volume and sample drying time. The measurement time and the sample volume on the carriers mainly affect the recovery rate and relative standard deviation of the quantified metal from aqueous solutions. The most important parameters that play a fundamental role in the calibration of a TXRF machine such as choice of the standard element and concentration ratio between the analyte and the standard are discussed. Practical and easy guidelines for the correct preparation of aqueous samples are presented. These can be used by both less and more experienced TXRF users, interested in measuring metal ion concentrations in aqueous samples.

© 2016 Elsevier B.V. All rights reserved.

1. Introduction

Total Reflection X-ray Fluorescence (TXRF) is an often used analytical technique for metal quantification in liquids, solids, wafers and biological samples [1–14]. Despite being amply referenced for the analysis of wafers, only recently benchtop TXRF spectrometers became commercially available and more competitive with techniques such as inductively coupled plasma optical emission spectroscopy (ICP-OES), inductively coupled plasma optical mass spectrometry (ICP-MS) or atomic absorption spectroscopy (AAS) [15–20]. This technique is very similar to Energy Dispersive X-ray Fluorescence (EDXRF) [7,21]. However, the relative position of the incident beam to the sample carrier is significantly different. In TXRF, the sample carrier is inclined under an angle of 0.1° with respect to the direction of the incident X-ray beam. This results in the total reflection of the X-ray beam on the surface of the sample carrier [21,22]. This total reflection of the X-ray beam has three main advantages: (1) the background signal is significantly reduced as almost no X-rays are penetrating into and exciting the sample carrier. The set-up geometry reduces the background and the detection limit by a factor of at least 10^3 depending on the element in comparison with EDXRF setups; (2) The sample on the carrier is excited by both the incident and the reflected beam, which results in an increased excitation probability of the sample elements, and (3) the carrier is placed very close to the detector (≈0.5 mm) which makes it able to collect a large amount of the fluorescence radiation of the sample [7]. In this way, the signal-to-noise ratio is low and concentrations into the ppb range can be measured.

The TXRF technique has several advantages over atomic absorption spectroscopy (AAS), instrumental neutron activation analysis (INAA) and techniques based on inductive coupled plasma (ICP-MS, ICP-OES). In TXRF, only a small amount of sample and chemicals are required for sample analysis, the sample preparation procedure is faster and the cost related to the measurements is much lower. Furthermore, different metals can be quantified in one single measurement and calibration curves are not compulsory for each measurement because element quantification can be performed by using an internal standard [7,23–25].

Despite its advantages, TXRF is not commonly used yet as a replacement for ICP methods or AAS [26]. This is probably due to its more recent development [27,28], the lack of standardization procedures (*i.e.* standardization by ISO, ASTM, or DIN has just started being developed) [23,29–31], and the influence of the sample preparation procedure on the accuracy and precision of the data [4,32,33]. In other techniques, the way and position in which the sample is entering the measurement unit is fixed and automated. In the case of TXRF measurements, the operator influences more directly the size, morphology and thickness of the sample and its position relative to the detector and the X-ray beam, aspects which can significantly influence the results.

Although several reviews, books and articles about TXRF have been published [6,21–23,26–28,33–37], there is a lack of fundamental, simple guidelines and standard procedures for new TXRF users who would like to apply the TXRF technique for measuring on liquid samples [7,21,27]. To date, our lab is using on a routine basis three TXRF machines (Picofox

* Corresponding author.
E-mail address: Tom.Vanderhoogerstraete@kuleuven.be (T. Vander Hoogerstraete).

http://dx.doi.org/10.1016/j.sab.2016.09.001
0584-8547/© 2016 Elsevier B.V. All rights reserved.

S2, Bruker) to quantify elemental concentration in up to 500 liquid samples every week. In this paper, a series of experiments are reported indicating that the sample preparation procedure is a key aspect on TXRF analysis. This paper does not focus on the technique itself, but on the practical side of performing TXRF measurements. The following questions are considered: (1) What is the influence of measuring time, sample position and the hard and software on the measurements? (2) How can highly reproducible data be obtained and what can be considered as the best sample preparation procedure? (3) How should the calibration of the machine be performed and when is it needed to be careful while processing results based on internal calibration? (4) How to clean sample carriers and what kind of impurities can be expected even after a proper cleaning procedure?

2. Experimental

2.1. Chemicals and equipment

The 1000 ± 10 mg L^{-1} praseodymium, neodymium and gallium (Pr, Nd and Ga) standards solutions were all obtained from Merck (Overijse, Belgium). A silicone solution in isopropanol was obtained from SERVA Electrophoresis GmbH (Heidelberg, Germany).

All TXRF measurements were performed with a benchtop Total Reflection X-ray Fluorescence (TXRF) spectrometer (Picofox S2, Bruker) operating with a molybdenum X-ray source at 50 kV. Reusable quartz sample carriers (4×30 mm) were employed for all measurements. The optimized sample preparation was the following: Firstly, the sample carriers were pretreated with 30 μL of silicone in isopropanol at room temperature and dried for 20 min in a hot air oven at 60 °C. This procedure was followed to make the surface hydrophobic and avoid spreading of the aqueous sample on the carrier. Secondly, 5 μL of the sample was added onto the carrier at room temperature and dried at 60 °C in a hot air oven for 30 min. The gain correction was performed before each series of measurements. Samples were measured for 200 s unless reported otherwise. All volumes were controlled gravimetrically by weighing. Spectra were analyzed with the Bruker Spectra Picofox V 7.5.3.0 software. Corrections were made for the escape peak, for pile ups and the background was corrected by a maximum of 1000 stripping cycles with a step width of 50. Samples were diluted with MilliQ water. Two identical TXRF machines (referred to in this study as TXRF1 and TXRF2) were tested to exclude effects specific to one of the machines and to validate, when necessary, the general conclusions for this type of machines.

The influence of the measuring time was studied by pipetting 5 μL of a solution containing 100 mg L^{-1} Ga and 100 mg L^{-1} of Nd on a sample carrier. The carrier was measured for different times, without any other manipulation, and the relative standard deviation (RR) was calculated based on three measurements at the specific time interval. This experiment was performed once on TXRF1 and twice on TXRF2.

The position of the sample carrier with respect to the X-ray beam was studied by pipetting 5 μL of a solution containing 100 mg L^{-1} Ga and 100 mg L^{-1} Nd onto six different carriers. Each sample was measured six times for 200 s without removing it from the measurement position and another six times with removal from the machine in between measurements. In another experiment, three sample carriers prepared with 5 μL of the former solution were measured under different positions relative to the X-ray beam. After each measurement of 200 s, the three different samples were rotated 60° and re-measured.

The influence of the drying time of the silicone in isopropanol, added on the sample carrier before addition of the sample, was studied by adding 30 μL of this solution on the sample carriers and drying it for different times at room temperature. After the specific drying time, 3 μL of a solution containing 100 mg L^{-1} Ga and 100 mg L^{-1} Nd was added onto the carrier and dried for 30 min in an oven at 60 °C. For the optimization of the sample amount, the sample carriers were pretreated with 30 μL of silicone solution and dried for 20 min in the oven at 60 °C. Afterwards, they were cooled to room temperature, and 1, 3 or 5 μL of a solution containing 100 mg L^{-1} Ga and 100 mg L^{-1} Nd was added, the carriers were dried for 20 min at 60 °C in a hot air oven. Nine series of ten measurements were performed. The influence of the sample drying time was studied on three different carriers containing a sample of 100 mg L^{-1} Ga and 100 mg L^{-1} Nd, the carriers were pretreated using the optimized procedure. The three samples were first measured when it was observed that all the water was evaporated from the sample. Afterwards, the sample was dried again for 5, 10, 15, 30, 45 and 60 min and measured immediately after each drying period. The RSD values at t_n are calculated based on the concentration values found in t_{n-1}, t_n and t_{n+1}.

The optimized sample procedure was tested by three different operators on six different days. The average count ratio of all measurements between Ga and Nd was used as the calibration factor. The non-linearity of the calibration factor was studied by preparing 12 different solutions containing all 100 mg L^{-1} Ga and different concentrations of Pr ranging between 1 and 900 mg L^{-1}. The sample carriers were pretreated as described above, and measured for 300 s. The 12 solutions were diluted a 10 fold and measured again for 3000 s to study the influence of possible matrix effects.

2.2. Formulas

The relative standard deviation (RSD) was calculated based on the following equation:

$$\mathrm{RSD}\ (\%) = \frac{\sqrt{\frac{\sum_{i=1}^{N} (x_i - \overline{x})^2}{N-1}}}{\overline{x}} \times 100 \quad (1)$$

where $\overline{x}$ is the average concentration, x_i the calculated concentration for measurement i and N the number of measurements.

The recovery rate (RR) is defined as:

$$RR\ (\%) = \frac{Measured\ concentration}{Expected\ concentration} \times 100 \quad (2)$$

3. Results

3.1. Parameter studies and optimization

All experiments were performed with Ga and the lanthanides Pr and Nd. Ga is often used as an internal standard in TXRF measurements because it is rarely found in aqueous samples. Lanthanides were chosen over more conventional and typically analyzed first row transition metals because the latter ones can be found in natural waters (Fe, Cu, Zn) or are sometimes difficult to remove from the sample carriers during the cleaning procedure (Fe, Zn). Both situations can influence the measurements, especially when working at low concentrations.

The measurement time has a relevant influence on the RSDs of the TXRF measurements (Fig. 1). A 5 μL sample of 100 mg L^{-1} Ga and 100 mg L^{-1} Nd was measured during different times. The RSD was calculated based on three measurements at each measurement time. All measuring times longer than 15 s gave RSDs smaller than 1%. All proceeding measurements were therefore performed for 200 s or longer in order to minimize the influence of the measuring time on the relative standard deviations. Note that the RSD values are directly depending on the number of counts rather than the measuring time. However, the use of counts rather than time is rarely done for TXRF machines requiring high sample throughput because of the uncertainty in effective measuring time and sample throughput.

After each measurement, the sample is removed mechanically from the measuring position by an automated gripper that rolls the sample carrier back into the sample holder. The relative position of the sample

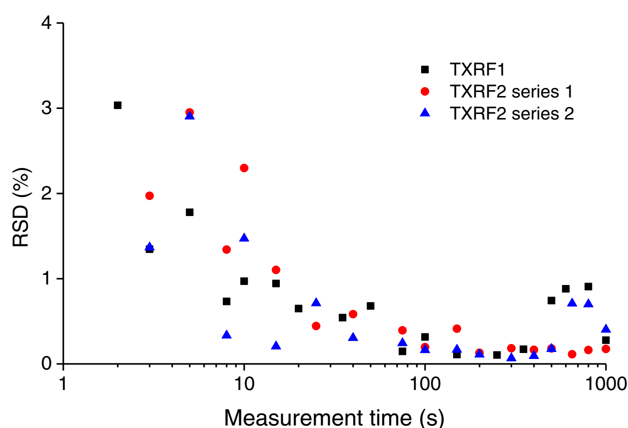

Fig. 1. Influence of the measurement time on the relative standard deviation (RSD) of the Nd concentration. (■): Experiments performed on TXRF1, (●) and (▲): experiments performed on TXRF2 in two different days. The RSD values are calculated based on a triplicate. 5 μL of a solution containing 100 mg L^{-1} Ga and 100 mg L^{-1} Nd standard was sampled on a TXRF carrier giving an average count rate of 8500 counts per second.

to the detector was therefore slightly different when the gripper placed the carrier back into the measuring position. Such rotation did not occur in the previously performed measurements. Therefore, the influence of such a rotation on the measurement was evaluated as described in the experimental section. The difference in RSD between removing and not removing the sample from the measurement position is very small (Table 1). Moreover, the RSD values are in the range found for the time experiments.

The next investigated parameter was the position of the sample carrier chosen by the operator. There are an infinite number of possible positions in which the sample carrier can be placed in the measuring position. The orientation of the sample relative to the ingoing and outgoing beam could also influence the results. Following the standard procedure, 5 μL of a solution containing 100 mg L^{-1} Ga and 100 mg L^{-1} Nd was disposed on a quartz sample carrier and measured for 200 s. After the measurement, the sample was rotated in the sample holder by 60°. This procedure was done in triplicate and repeated six times until the three carriers were back in their initial position. The RSDs on these measurements were 0.27, 0.30 and 0.52%. These values are slightly higher than the average RSD values reported in Table 1. However, it can be seen in Fig. 1 that such RSD values can be expected even without changing the position of the sample. Therefore, random errors introduced by the sample position are negligible in comparison with the effect of the measuring time.

Pipettes may cause random errors during the sample preparation procedure as well, but such errors are often smaller than 0.6%. Systematic errors are avoided by using the same pipette and an internal standard. It is important to mention that errors made by pipetting were avoided in this work by performing most of the experiments from one single mixed metal ion stock solution and by controlling and correcting the volumes gravimetrically. Next, the sample preparation method was

Table 1
Relative standard deviation (RSD) made on the measurement of six sample carriers sampled with 5 μL of 100 mg L^{-1} Ga and 100 mg L^{-1} of Nd that were measured with and without removal from the measurement position (position change).

Carrier	Without position change	With position change
	RSD (%)	RSD (%)
1	0.20	0.65
2	0.22	0.25
3	0.16	0.39
4	0.79	0.15
5	0.13	0.08
6	0.18	0.24
Average	0.28	0.29

optimized in which (1) the amount, drying time and temperature of silicone in isopropanol were studied as well as (2) the amount, drying time and temperature of the sample on the siliconized carrier. In contrast to poly(methyl methacrylate) (PMMA), quartz glass is not hydrophobic, but can be made hydrophobic by treating it with a silicone solution. From experience, we know that the volume of silicone in isopropanol solution, covering the whole TXRF carrier needs to be at least 30 μL at room temperature. Addition of the silicone solution to a carrier at higher temperature results often in migration of the solution to one side of the carrier and an inhomogeneous spreading of the silicone solution over the carrier. This can cause a movement of the sample droplet over the carrier resulting in significant errors in the measurement [38].

Volumes smaller than 30 μL but at room temperature are also spread out inhomogeneously over the carrier, especially in the case of older sample carriers, which could have some scratches on their surface. The drying time of the silicone solution in isopropanol at 60 °C was varied between 30 and 240 min. Each data point represents the RSD on 10 sample carriers prepared at different moments with 3 μL of a solution containing 100 mg L^{-1} Ga and 100 mg L^{-1} Nd (Fig. 2). There is a slight decrease in the RSDs when the silicone solution in isopropanol was dried for a longer time, however, all RSDs remained below 2% and therefore, the drying time of the silicone in isopropanol at 60 °C does not have a significant effect on the reproducibility and accuracy of the measurements.

Next, the amount of sample on the sample carrier was investigated. An aliquot of 1, 3 or 5 μL of a solution containing 100 mg L^{-1} Ga and 100 mg L^{-1} Nd was added on a carrier pretreated with silicone in isopropanol. Three series of 10 samples carriers with 1, 3 or 5 μL of sample were prepared at different moments. To keep the number of counts approximately constant, the measurement time was increased when decreasing the sample volume, thus, sample volumes of 1 μL were measured during 1000 s, sample volumes of 3 μL during 333 s and sample volumes of 5 μL during 200 s. As it can be seen in Fig. 3, there is a general trend of decreasing RSD values while decreasing the amount of sample. At lower volumes the droplet has less chance to move on the carrier and it remains in the center.

The drying time of the sample was studied as well. Therefore, a triplicate of sample carriers containing 5 μL of a solution with 100 mg L^{-1} Ga and 100 mg L^{-1} Nd was prepared. The samples were measured when it was seen that all water had been removed from the sample by drying it in the oven ($t = 0$ min). After the measurement, the sample was placed again into the oven for a specific time interval and measured again. This sequence was followed after 5, 10, 15, 30, 45, 60 and

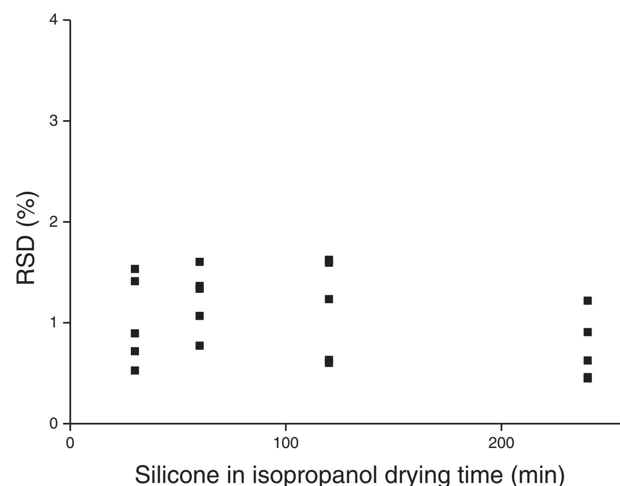

Fig. 2. Relative standard deviation (RSD) on the measurement of 10 sample carriers containing 3 μL of a solution with 100 mg L^{-1} Ga and 100 mg L^{-1} Nd as function of the drying time of silicone in isopropanol. Drying at 60 °C with a measurement time of 333 s.

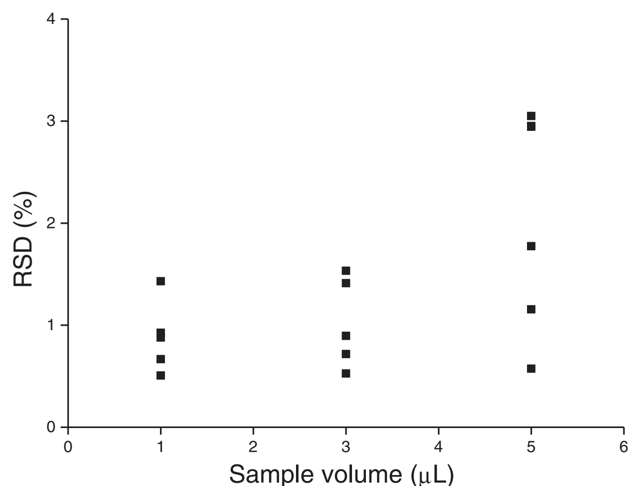

Fig. 3. Influence of the sample volume pipetted on the carrier on the RSD values for the recovery of Nd. 5 times 10 sample carriers sampled with different volumes of a solution containing 100 mg L^{-1} Ga and 100 mg L^{-1} Nd were measured at each volume.

960 min. It was shown before that the effect of the software, counting statistic and the sample position gave RSD values around 0.3% (Table 1, Fig. 1 and the discussions). The RSD values given in Fig. 4 at time t_n are calculated based on the concentration values found in t_{n-1}, t_n and t_{n+1}. RSD values are in most cases significantly higher. This is probably more an effect of re-drying rather than an effect of drying time. After each drying procedure at 60 °C, the dried sample is cooled down to room temperature. As most samples contain mainly hygroscopic salts, they can take up water from the air and even become (partly) liquid. A re-drying process can cause recrystallization processes which mainly occur at places already enriched in this specific element, causing a non-uniformity across the sample affecting the accuracy of a quantitative analysis. The evaporation behavior of different kinds of droplets and studies on their morphology and homogeneity once dried have been studied and reported elsewhere [7,39–41]. In TXRF, the superposition or interference between the incoming and reflected beams at small grazing incidence angles can cause X-ray standing waves above and below the substrates. The effect of these standing waves is usually not taken into account since two assumptions are made: first, the lateral inhomogeneity of the X-ray standing wave field is averaged in the measured signal and second, that both sample and standard are homogeneously distributed [42–44]. However, if irregular aggregates

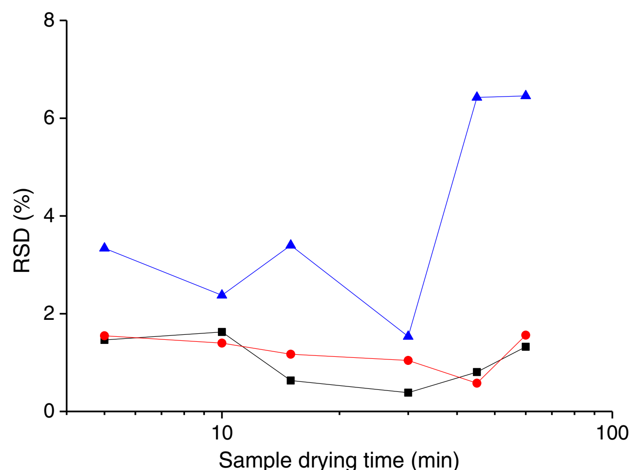

Fig. 4. Influence of the sample drying time on the RSD values of 3 samples containing 100 mg L^{-1} Ga and 100 mg L^{-1} Nd. The RSD values shown at time t_n are calculated based on the concentration values found in t_{n-1}, t_n and t_{n+1}. Note that the X-axis is plotted on a logarithmic scale.

of analyte or standard are present at different points of the sample, the interference between the incoming and reflected waves cannot occur, destroying the X-ray wave field and therefore, affecting the intensity of the detected fluorescence [42,45]. Other possibilities could be the loss of material during sample preparation (although significant decreases in count rates are not observed) or decreased matrix effects by further reducing the amount of (crystal) water when drying for longer period. Even significant higher RSD values and recovery rates are observed when drying the silicone solution in isopropanol at 60 °C for only 2 min and obtaining a sample residue covering a larger surface area on the carrier.

The most important parameters influencing the standard deviations on TXRF measurements were investigated for samples containing 100 mg L^{-1} Ga and 100 mg L^{-1} Nd. The next step was to test if other operators could find the same results (%RR and RSD) when following the same procedure. Table 2 gives an overview of six series of 10 measurements performed on different days and by different operators. The results show a very high accuracy and reproducibility of all measurements.

3.2. Calibration curves

So far, only solutions having equal Nd and Ga mass concentrations (100 mg L^{-1}) have been measured. Such conditions are rarely faced when measuring real samples with elements present in unknown concentrations. A straightforward and correct calibration method for TXRF measurements with an internal standard is of high importance. Ideally, the calibration is valid for a wide range of concentrations relative to the internal standard that is used. The calibration factor gives the ratio of the detected X-ray fluorescence intensity from an internal standard element relative to the element of interest at equal concentrations. In order to check the linearity of this calibration factor, a series of 12 calibration solutions containing 100 mg L^{-1} Ga and different amounts of Pr ranging from 1 to 900 mg L^{-1} were prepared (Fig. 5). All data were normalized to the recovery rate found for 100 mg L^{-1} Ga and 100 mg L^{-1} Pr.

In Fig. 5, the red dots represent the results obtained with the more concentrated solutions. There is a Pr concentration overestimation at Pr concentrations that are relatively low compared to Ga and an underestimation of the Pr concentration at Pr concentrations that are relatively high compared to Ga. This non linearity in counts and recovery rate is remarkable as one of the fundamental assumptions of TXRF is that the number of counts of an element is proportional to its concentration. Moreover, these results suggest that TXRF measurements need to be performed in a very narrow, calibrated concentration range and that quite often large errors are made when using a single internal standard for quantifying multi-element solutions containing metals present in different concentrations. The graph can be split into three regions when considering the standard deviations. The standard deviation is high on the left hand side of the graph which is due to the lower detected X-ray fluorescence intensity resulting in a lower signal to noise ratio and a larger uncertainty on the peak intensity. On the right hand side, the concentrations are relatively high and matrix effects start to play a role. Therefore, the standard deviations are again higher. The standard

Table 2
Recovery rates and RSD values on 6 series of 10 measurements with 1 μL solution containing 100 mg L^{-1} Ga and 100 mg L^{-1} Nd measured by three different operators at six different days.

Day	Operator	RR (%)	RSD (%)
1	A	101.8	1.4
2	A	102.2	0.7
3	B	101.2	0.8
4	B	101.4	1.4
5	C	99.9	1.3
6	C	101.5	1.1

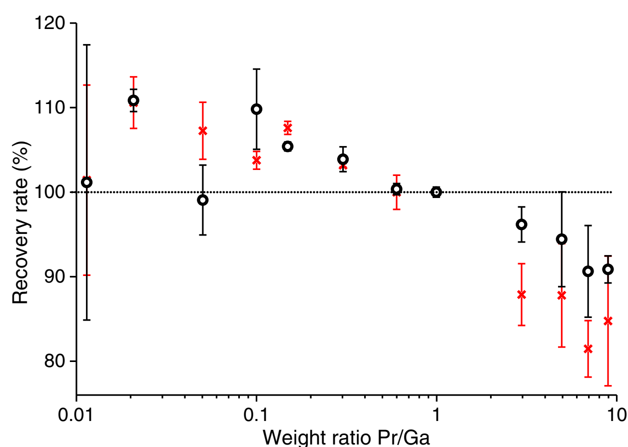

Fig. 5. Pr recovery rate (%) as function of the mass ratio Pr/Ga in the solution. Red = 100 mg L^{-1} Ga, Black = the red solutions 10 times diluted (10 mg L^{-1} Ga). Each data point was measured in triplicate. Note that the X-axis is plotted on a logarithmic scale. Error bars represent the standard deviation. (For interpretation of the references to colour in this figure legend, the reader is referred to the web version of this article.)

deviation is low at medium concentrations (around a Pr/Ga mass ratio of 1 and with a gallium concentration of 100 mg L^{-1}). Afterwards, the 12 solutions were diluted a tenfold (to a Ga concentration of 10 mg L^{-1}) to prove that this non-linearity is not caused by the fact that relative large metal concentrations are used. The measuring time was increased from 300 s to 3000 s in order to get a similar detected X-ray fluorescence intensity for the elements of interest. The black curve in Fig. 5 shows a similar trend although the recovery rates are closer to 100% at higher Pr concentrations.

This non-linearity when using Ga as internal standard was also observed with other rare earths and transition metals. Nd and Pr are two lanthanides having L-lines with very close energies. The effect on the recovery rates, as shown in Fig. 6, is very similar suggesting that, when measuring Nd, Pr should be a better internal standard, canceling out the effect that causes the non-linearity shown in Fig. 5. Therefore, a similar experiment was carried out in which the Pr concentration was kept at 100 mg L^{-1} and the Nd concentration was varied. Fig. 6 shows that indeed, the recovery rates and standard deviations are much better than in the case of Pr/Ga, however, at low Pr/Nd ratios, the peaks of Pr are overlapping more the peaks of Nd making difficult to distinguish them, resulting in lower recovery rates for Pr.

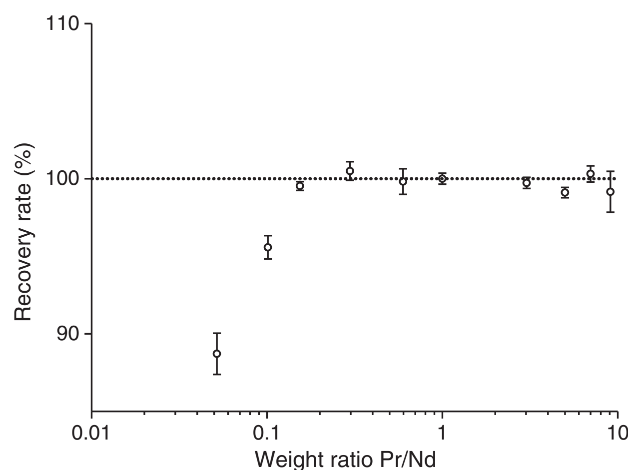

Fig. 6. Pr recovery rate (%) as function of the mass ratio Nd/Pr in solution. Pr concentration: 100 mg L^{-1}, each data point was measured in triplicate. Note that the X-axis is plotted on a logarithmic scale. Error bars represent the standard deviation.

Therefore, to get accurate and precise data, the calibration of the elements is performed by measuring 10 times a mixture of the element of interest and gallium as internal standard at equal concentrations (100 mg L^{-1}). Often, the calibration of the TXRF machines is carried out by making groups of four or five metals for which the X-rays are not overlapping and with concentrations of 50 mg L^{-1} to avoid matrix effects. In the case of single-element solutions is strongly suggested to re-measure a solution if the element of interest is less than half or more than double of the concentration of the internal standard used and, if possible, to measure with an internal standard that has an X-ray fluorescence energy as close as possible to the element of interest. For multi-element solutions with extremely different concentrations, it is recommended to evaluate the best conditions for the measurements in terms of the choice of the internal standard element and its concentration.

3.3. Carrier, blank problems and detector contamination

One of the most sensitive and expensive parts of a TXRF machine is the detector. Depending on the nature of the detector, problems due to corrosion can be faced when exposed to corrosive gases. The center of the detector shown in Fig. 7 is damaged and the surroundings suggest that volatile species escape from the matrix and condense on the detector assembly. First of all, improper drying of the sample can conduce to samples that still contain significant amounts of acid like HNO_3 (which comes from the internal standards used). During the measurement, it is possible that part of the remaining acid evaporates and condenses on the detector. However, it is very unlikely that still significant amounts of HNO_3 evaporate at room temperature after a drying procedure of 30 min at 60 °C. It is more likely that high chloride salt matrices are causing the corrosion. Samples with (high) chloride matrices (*e.g.* NaCl, NH_4Cl, $CaCl_2$, *etc.*) need special attention since these hygroscopic salts can take up water from the air when standing in the sample holder, waiting to be measured. Metal salts present in the sample can hydrolyze and release highly volatile HCl gas that condenses on the detector. A way to change from a chloride to a nitrate matrix is adding a small quantity (*e.g.* 0.005 mL) of 68 wt% HNO_3 acid onto the residue that remains after drying. The removal of chloride from a 1.1 M solution of $CaCl_2$ was tested. By drying the chloride solution again in combination with HNO_3 in a hot air oven at elevated temperatures, chloride ions are oxidized by the nitrate ions and the chlorine gas that is formed escapes from the sample before mounting the carrier into the TXRF machine, the chloride recovery rate was 0.005%.

The expensive quartz sample carriers can be cleaned after usage. However, it is sometimes difficult to get a clean spectrum and often contaminations are observed, especially when measuring into the low ppm or ppb range. Also old TXRF carriers often have metal impurities left in scratches on the carrier surface. Apart from the known elemental

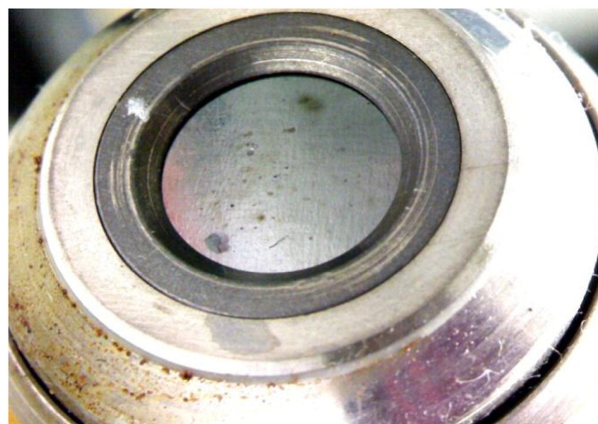

Fig. 7. Contamination and corrosion of the detector window (10 mm^2).

peaks of molybdenum (source), argon (air) and silicon (in case of a quartz carrier), other impurities that can frequently be observed in the spectrum are calcium, zinc, iron, lead and other elements depending on the type of samples analyzed. When the cleaning of the carriers is not performed properly, stable oxides of these elements can be formed which are difficult to be removed, and which interfere with the analysis. For these reasons, it is recommended to use the following cleaning procedure: (1) cleaning with water and a lint-free cleaning tissue to remove salts, (2) cleaning with acetone and a lint-free cleaning tissue to remove silicone or organic material from the carrier, (3) loading the washing cassette with the pre-cleaned sample carriers, placing the cassette inside a covered beaker and heating it with a 3 wt% HCl solution during half an hour to remove metals and especially Fe(III) and Pb(II), (4) rinsing the sample carriers with distilled water and heating the cassette with RBS 50 pF during half an hour to dissolve the silicone on the carrier, (5) rinsing the sample carriers with distilled water and heating with HNO_3 during two hours to remove the remaining metal impurities, (6) rinsing with MilliQ water, (7) rinsing with acetone, (8) drying the sample carriers in the cassette at 60 °C during half an hour, (9) placing 30 μL of silicone solution onto the sample carrier and drying them during half an hour at 60 °C, and finally (10) measuring each sample carrier during 200 s to check their cleanness.

4. Conclusions

To illustrate the relevance of sample preparation in the detection and quantification of aqueous metal ion solutions by TXRF, different important parameters such as choice of standard, sample volume, drying time, measurement time and the calibration have been studied and discussed. As a result, optimal conditions needed for the correct measurement of metal ion solutions by TXRF were found and practical and simple guidelines were formulated which can improve the quality, reliability and accuracy of the measurements. For example, better results are obtained when the internal standard and the analyte have closer X-ray line energies, which is in contrast with the common practice to use gallium as the only internal standard. The concentration ratio of the standard should be close to the one of the analyte in the sample in order to assure good recovery rates. The quality of the analysis can be improved, for instance, by using smaller sample volumes in order to avoid movement of the droplet on the carrier. Further experiments are being carried out to address complex matrix effects (*e.g.* ionic liquids, high salt content) which will be addressed in a future publication.

Acknowledgements

The research leading to these results has received funding from the European Community's Seventh Framework Programme ([FP7/2007–2013]) under grant agreement no. 607411 (MC-ITN EREAN: European Rare Earth Magnet Recycling Network). This publication reflects only the author's view, exempting the Community from any liability. Project website: http://www.erean.eu. In addition, partial funding was received from the European Community's Seventh Framework Programme ([FP7/2007-2013], EURARE) under grant agreement n°309373. Project website: http://www.eurare.eu/. The authors also thank the KU Leuven for funding GOA/13/008 and IOF-KP RARE^3). TVDH thanks the FWO Flanders for a postdoctoral fellowship. The authors thank Armin Gross, Hagen Stosnach and Ulrich Waldschlaeger (Bruker, Berlin) for their time and the fruitful discussions.

References

[1] E.K. Towett, K.D. Shepherd, G. Cadisch, Quantification of total element concentrations in soils using total X-ray fluorescence spectroscopy (TXRF), Sci. Total Environ. 463–464 (2013) 374–388.
[2] T. Vander Hoogerstraete, S. Jamar, S. Wellens, K. Binnemans, Determination of halide ions in solution by Total Reflection X-ray Fluorescence (TXRF) spectrometry, Anal. Chem. 86 (2014) 1391–1394.
[3] T. Vander Hoogerstraete, S. Jamar, S. Wellens, K. Binnemans, Determination of halide impurities in ionic liquids by total reflection X-ray fluorescence spectrometry, Anal. Chem. 86 (2014) 3931–3938.
[4] S. Pahlke, L. Fabry, L. Kotz, C. Mantler, T. Ehmann, Determination of ultra trace contaminants on silicon wafer surfaces using total-reflection X-ray fluorescence TXRF 'state-of-the-art', Spectrochim. Acta B 56 (2001) 2261–2274.
[5] F.R. Espinoza-Quiñones, A.N. Módenes, S.M. Palácio, N. Szymanski, R.A. Welter, M.A. Rizzutto, et al., Evaluation of trace element levels in muscles, liver and gonad of fish species from São Francisco River of the Paraná Brazilian state by using SR-TXRF technique, Appl. Radiat. Isot. 68 (2010) 2202–2207.
[6] M. Mages, S. Woelfl, M. Óvári, W.V. Tümpling Jun, The use of a portable total reflection X-ray fluorescence spectrometer for field investigation, Spectrochim. Acta B 58 (2003) 2129–2138.
[7] R.V.B. Klockenkämper, Total-Reflection X-Ray Fluorescence Analysis and Related Methods, John Wiley & Sons, New Jersey, 2015.
[8] R. Sitko, P. Janik, B. Zawisza, E. Talik, E. Margui, I. Queralt, Green approach for ultratrace determination of divalent metal ions and arsenic species using Total-Reflection X-ray Fluorescence spectrometry and mercapto-modified graphene oxide nanosheets as a novel adsorbent, Anal. Chem. 87 (2015) 3535–3542.
[9] M. Menzel, U.E.A. Fittschen, Total reflection X-ray fluorescence analysis of airborne silver nanoparticles from fabrics, Anal. Chem. 86 (2014) 3053–3059.
[10] R. Fernández-Ruiz, M.J. Redrejo, E.J. Friedrich, M. Ramos, T. Fernández, Evaluation of bioaccumulation kinetics of gold nanorods in vital mammalian organs by means of total reflection X-ray fluorescence spectrometry, Anal. Chem. 86 (2014) 7383–7390.
[11] S. Kunimura, J. Kawai, Portable total reflection X-ray fluorescence spectrometer for nanogram Cr detection limit, Anal. Chem. 79 (2007) 2593–2595.
[12] V.S. Hatzistavros, N.G. Kallithrakas-Kontos, Determination of trace perchlorate concentrations by anion-selective membranes and total reflection X-ray fluorescence analysis, Anal. Chem. 83 (2011) 3386–3391.
[13] C. Neumann, P. Eichinger, Ultra-trace analysis of metallic contaminations on silicon wafer surfaces by vapour phase decomposition/total reflection X-ray fluorescence (VPD/TXRF), Spectrochim. Acta B 46 (1991) 1369–1377.
[14] M.L. Carvalho, T. Magalhães, M. Becker, A. von Bohlen, Trace elements in human cancerous and healthy tissues: a comparative study by EDXRF, TXRF, synchrotron radiation and PIXE, Spectrochim. Acta B 62 (2007) 1004–1011.
[15] L. Borgese, F. Bilo, K. Tsuji, R. Fernández-Ruiz, E. Margui, C. Streli, et al., First total reflection X-ray fluorescence round-robin test of water samples: preliminary results, Spectrochim. Acta B 101 (2014) 6–14.
[16] L. Borgese, F. Bilo, R. Dalipi, E. Bontempi, L.E. Depero, Total reflection X-ray fluorescence as a tool for food screening, Spectrochim. Acta B 113 (2015) 1–15.
[17] H. Stosnach, On-site analysis of heavy metal contaminated areas by means of total reflection X-ray fluorescence analysis (TXRF), Spectrochim. Acta B 61 (2006) 1141–1145.
[18] R. Dalipi, E. Marguí, L. Borgese, F. Bilo, L.E. Depero, Analytical performance of benchtop total reflection X-ray fluorescence instrumentation for multielemental analysis of wine samples, Spectrochim. Acta B 120 (2016) 37–43.
[19] H. Stosnach, Environmental trace-element analysis using a benchtop total reflection X-ray fluorescence spectrometer, Analyt. Sci 21 (2005) 873–876.
[20] E. Marguí, J.C. Tapias, A. Casas, M. Hidalgo, I. Queralt, Analysis of inlet and outlet industrial wastewater effluents by means of benchtop total reflection X-ray fluorescence spectrometry, Chemosphere 80 (2010) 263–270.
[21] P. Wobrauschek, Total reflection X-ray fluorescence analysis—a review, X-Ray Spectrom. 36 (2007) 289–300.
[22] H. Aiginger, Historical development and principles of total reflection X-ray fluorescence analysis (TXRF), Spectrochim. Acta B 46 (1991) 1313–1321.
[23] R. Klockenkämper, A. von Bohlen, Worldwide distribution of total reflection X-ray fluorescence instrumentation and its different fields of application: a survey, Spectrochim. Acta B 99 (2014) 133–137.
[24] I. De La Calle, N. Cabaleiro, V. Romero, I. Lavilla, C. Bendicho, Sample pretreatment strategies for total reflection X-ray fluorescence analysis: a tutorial review, Spectrochim. Acta B 90 (2013) 23–54.
[25] N.H. Bings, A. Bogaerts, J.A.C. Broekaert, Atomic spectroscopy: a review, Anal. Chem. 82 (2010) 4653–4681.
[26] R. Klockenkämper, Challenges of total reflection X-ray fluorescence for surface- and thin-layer analysis, spectrochim, Acta Part B 61 (2006) 1082–1090.
[27] Y. Yoneda, T. Horiuchi, Optical flats for use in X-ray spectrochemical microanalysis, Rev Sci Instrum 42 (1971) 169–170.
[28] P. Wobrauschek, H. Aiginger, Total-reflection X-ray fluorescence spectrometric determination of elements in nanogram amounts, Anal. Chem. 47 (1975) 852–855.
[29] ISO18507, Surface Chemical Analysis. Use of Total Reflection X-ray Fluorescence Spectroscopy in Biological and Environmental Analysis, 2015.
[30] ISO14706, Surface Chemical Analysis - Determination of Surface Elemental Contamination on Silicon Wafers by Total-Reflection X-ray Fluorescence (TXRF) Spectroscopy, 2014.
[31] ISO17331, Surface Chemical Analysis. Chemical Methods for the Collection of Elements From the Surface of Silicon-Wafer Working Reference Materials and Their Determination by Total-Reflection X-ray Fluorescence (TXRF) Spectroscopy, 2004.
[32] G.H. Floor, I. Queralt, M. Hidalgo, E. Marguí, Measurement uncertainty in Total Reflection X-ray Fluorescence, Spectrochim. Acta B 111 (2015) 30–37.
[33] A. Prange, U. Reus, H. Schwenke, J. Knoth, Optimization of TXRF measurements by variable incident angles, Spectrochim. Acta B 54 (1999) 1505–1511.
[34] M. Schmeling, X-ray Fluorescence and Emission | Total Reflection X-ray Fluorescence, Elsevier, 2013.
[35] N.V. Alov, Total reflection X-ray fluorescence analysis: physical foundations and analytical application (a review), Inorg. Mater. 47 (2011) 1487–1499.

[36] D. Hampai, S.B. Dabagov, C. Polese, A. Liedl, G. Cappuccio, Laboratory total reflection X-ray fluorescence analysis for low concentration samples, Spectrochim. Acta B 101 (2014) 114–117.
[37] R. Klockenkàmper, J. Knoth, A. Prange, H. Schwenke, Total-reflection X-ray fluorescence spectroscopy, Anal. Chem. 64 (1992) 1115A–1123A.
[38] Y. Tabuchi, K. Tsuji, TXRF intensity dependence on position of dried residue on sample carrier and TXRF determination of halogen in liquid samples, X-Ray Spectrom. (2016), http://dx.doi.org/10.1002/xrs.2688.
[39] M. Menzel, O. Scharf, S.H. Nowak, M. Radtke, U. Reinholz, P. Hischenhuber, et al., Shading in TXRF: calculations and experimental validation using a color X-ray camera, J. Anal. At. Spectrom. 30 (2015) 2184–2193.
[40] J.K. Park, J. Ryu, B.C. Koo, S. Lee, K.H. Kang, How the change of contact angle occurs for an evaporating droplet: effect of impurity and attached water films, Soft Matter 8 (2012) 11889–11896.
[41] A. Marin, R. Liepelt, M. Rossi, C.J. Kahler, Surfactant-driven flow transitions in evaporating droplets, Soft Matter 12 (2016) 1593–1600.
[42] D.K.G. de Boer, X-ray standing waves and the critical sample thickness for total-reflection, Spectrochim. Acta B 46 (1991) 1433–1436.
[43] M. Kramer, A. von Bohlen, C. Sternemann, M. Paulus, R. Hergenröder, Synchrotron radiation induced X-ray standing waves analysis of layered structures, Appl. Surf. Sci. 253 (2007) 3533–3542.
[44] M. Kramer, A. von Bohlen, C. Sternemann, M. Paulus, R. Hergenroder, X-ray standing waves: a method for thin layered systems, J. Anal. At. Spectrom. 21 (2006) 1136–1142.
[45] M. Kramer, T.H. Holz, D. Weiflbach, G. Falkenberg, R. Simon, U. Fittschen, T. Krugmann, M. Kolbe, M. Muller, B. Beckhoff, Ultrathin layer depositions - a new type of reference samples for high performance XRF analysis, Adv. X Ray. Anal 54 (2011) 209–304.